Published online 23 October 2016 *Nucleic Acids Research, 2016, Vol. 44, No. 21* ***10031–10041***
doi: 10.1093/nar/gkw947

Light-induced oxidation of the telomeric G4 DNA in complex with Zn(II) tetracarboxymethyl porphyrin

Artemy D. Beniaminov[1,*], Roman A. Novikov[1], Olga K. Mamaeva[1], Vladimir A. Mitkevich[1], Igor P. Smirnov[2], Mikhail A. Livshits[1], Anna K. Shchyolkina[1] and Dmitry N. Kaluzhny[1,*]

[1]Engelhardt Institute of Molecular Biology, Russian Academy of Sciences, Vavilov str., 32, 119991 Moscow, Russia and [2]Institute for Physical-Chemical Medicine of Ministry of Public Health, Malaya Pirogovskaya str. 1a, 119435 Moscow, Russia

Received June 29, 2016; Revised October 04, 2016; Editorial Decision October 07, 2016; Accepted October 10, 2016

ABSTRACT

Structure-specific ligands are convenient tools for the recognition, targeting or probing of non-canonical DNA structures. Porphyrin derivatives exhibit a preference for interaction with G-quadruplex (G4) structures over canonical duplex DNA and are able to cause photoinducible damage to nucleic acids. Here, we show that Zn(II) 5,10,15,20-tetrakis(N-carboxymethyl-4-pyridinium)porphyrin (ZnP1) interacts with different conformations of the telomeric sequence d(TAGGG(TTAGGG)$_3$) at submicromolar concentrations without any detectible disturbance of the particular fold. Among different folds, potassium (3+1) hybrid G4-structure. reveal the highest affinity to ZnP1. The pattern of guanine oxidation is specific for each telomeric DNA conformation and may serve as an additional tool for probing the G4 topology. The potassium (3+1) and parallel G4 conformations are more susceptible to light-induced oxidation than the sodium G4 conformation or double helix of the telomeric DNA. The major products of the guanine modifications are spiroiminodihydantoin (Sp) and 8-oxoguanine (8-oxoG). ZnP1-induced oxidation of guanines results in the structural rearrangement of parallel and (3+1) G4 conformations yielding an antiparallel-like G4 conformation. The mechanism of the observed light-induced conformational changes is discussed.

INTRODUCTION

Telomeric DNA is a promising target for small molecules in a potential antitumor therapy. Such therapy is aimed at the inhibition of the telomerase, a ribonucleoprotein, which is known to be activated in ∼90% of all human tumors (1). The very end of human telomeres consists of a single stranded hexanucleotide DNA repeat (TTAGGG)$_n$ that is capable of forming a G-quadruplex structure. Human telomeric DNA reveals extreme structural diversity *in vitro*. Several conformations of telomeric DNA were solved by NMR and X-ray techniques (2–9). In most conformations, all guanines are involved in the formation of G-quartets, however, 5′-3′ direction of each of the four strands may vary. Solution conditions as well as flanking nucleotides of an oligonucleotide determine the preferable G4 conformation. For example, the basket type of antiparallel G4 is formed by d(AGGG(TTAGGG)$_3$) in .NaCl solution (2). However, the same oligodeoxynucleotide in the presence of K+ ions revealed a propeller-type of all-parallel structure when solved by X-ray crystallography (3). A formation of (3+1) structures in K+ solution was observed with NMR. In that study, oligonucleotides d(TAGGG(TTAGGG)$_3$) and d(TAGGG(TTAGGG)$_3$TT) formed the structures named (3+1) Form 1 and (3+1) Form 2, respectively (4–6). Two other possible structures with (3+1) strand orientation were assumed to also exist (6). Wang *et al*. found that oligonucleotide d(TAGGG(TTAGGG)$_3$) in Na^+ solution also forms the (3+1) Form 1 structure despite different CD and 1D NMR spectra (7). The authors explained the differences in CD and NMR spectra between sodium Na+ and K+ structures of d(TAGGG(TTAGGG)$_3$) via different quartet stacking in varied cation conditions (7). Another basket type antiparallel G4 structure was observed for d(GGG(TTAGGG)$_3$T) in KCl solution and contained only two G-quartets (8). Different G-quadruplex conformations can be converted to a propeller-type parallel-stranded G-quadruplex in a water depleted potassium-containing crowded solution (9). Processes of G-quadruplex folding and interconversion between different conformation are being intensively studied (10,11).

Small molecules specific to G4 structures may have several important applications. Besides inhibition of the telomerase and cell growth arrest, these molecules can potentially be used in recognition and targeting the G4, G4 imaging,

*To whom correspondence should be addressed. Tel: +7 499 135 1255; Fax: +7 499 135 1405; Email: abeniaminov@mail.ru
Correspondence may also be addressed to Dmitry Kaluzhny.Tel: +7 499 135 1255; Fax: +7 499 135 1405; Email: uzhny@mail.ru

© The Author(s) 2016. Published by Oxford University Press on behalf of Nucleic Acids Research.
This is an Open Access article distributed under the terms of the Creative Commons Attribution License (http://creativecommons.org/licenses/by-nc/4.0/), which permits non-commercial re-use, distribution, and reproduction in any medium, provided the original work is properly cited. For commercial re-use, please contact journals.permissions@oup.com

directed suppression of genes containing G4 motifs and finally, as a structural probe of the G4 DNA. In the latter case, the influence of a G4 binder on the G4 conformation is of considerable importance. G4 specific ligands either stabilize the G4 structure and/or cause certain conformational rearrangements. Binding of some bisquinolinium G4 DNA ligands (360A, Phen-DC3 and pyridostatin) can result in the restructuring of telomeric G4 into an antiparallel two-quartets fold presumably due to the displacement of metal ions (12). The destruction of all quartets in the telomeric G4 structure in sodium or a single quartet in potassium is required for anthrathiophenedione derivative binding (13). These changes essentially depend on ligand binding and seem to be reversible upon ligand dissociation.

Porphyrin derivatives are generators of singlet oxygen, a characteristic property utilized in the photodynamic therapy (14). The oxidation pathways of the telomeric quadruplex triggered by several oxidative stress inducers were studied (15). It was found that singlet oxygen preferably oxidizes all guanines on the exterior faces of G-quartets and furnishes multiple products of oxidation including a major final product of spiroiminodihydantoin (Sp). Individual guanines were subject to oxidation in the telomeric quadruplex complex with TMPyP4 (16). Oxidation of guanines in the 5′-position of the GGG block reduces telomerase activity (17). Additionally, G-quadruplex structure hinders the removal of oxidative DNA lesions by human DNA glycosylases (18).

Cationic porphyrins bind with some preference to G4 over canonical double-stranded DNA structure (19,20). Tetracarboxymethyl porphyrins, including **ZnP1** (Supplementary Figure S1), were synthesized (21,22) and their DNA binding properties were described by us earlier (22–24). Here, we focus on the mechanism of the interaction between the **ZnP1** porphyrin and the telomeric sequence and its ability to light-induce oxidation of guanines within different G4 conformations. **ZnP1** revealed a high affinity to G4 structures, preference to certain G4 telomeric conformations and a high yield of guanine oxidation under light irradiation. All these features are useful in developing approaches for controllable reduction of telomerase activity in tumor cells.

The same properties of the **ZnP1** porphyrin are helpful in discriminating between various conformations of G4 DNA. Previously, well-studied cationic 5,10,15,20-tetrakis-(4-N-methylpyridiniumyl) porphyrin (TMPyP4) (25) as well as tetrakis(2-trimethylaminoethylethanol) phthalocyaninato zinc tetraiodine (Zn-TTAPc) (26) were used as singlet oxygen generating probes for determining strand orientation in different intramolecular folds of G4 structures. However, it was found that interaction of the indicated ligands with G- quadruplex led to considerable distortion of G4 conformation (20,26).

Here, we study the interaction and light-induced oxidation of the telomeric G-quadruplex with **ZnP1.** Binding of the **ZnP1** porphyrin to different folds of the telomeric quadruplex appears to retain its native G4 conformation, thus making **ZnP1** a more favorable agent for accurate probing of the highly polymorphic structure of the human telomeric DNA. Additionally, we demonstrate that prolonged light irradiation of the **ZnP1**:G4 complex results in changes of the G4 structure specific to its initial conformation.

MATERIALS AND METHODS

Chemicals and sample preparation

The oligodeoxynucleotides TQ23: TAGGG(TTAGGG)$_3$, TQ23-F: TAGGG(TTAGGG)$_3$-FAM, F-TQ23: FAM-TAGGG(TTAGGG)$_3$, TQ23comp: (CCCTAA)$_3$CCCTA, TQ22: AGGG(TTAGGG)$_3$, TQ22-F AGGG(TTAGGG)$_3$-FAM, nonG4: AGGCTTGGCGGGAAAAAGAACG-FAM were synthesized by DNA-synthesis (Moscow, Russia). The concentration of each oligonucleotide was determined spectrophotometrically based on absorption at 260 nm in water at 90°C using the following molar extinction coefficients: ϵ(TQ23) = 269 000 $M^{-1}\cdot cm^{-1}$ and ϵ(TQ23comp) = 233 000 $M^{-1}\cdot cm^{-1}$, ϵ(TQ22) = 261000 $M^{-1}\cdot cm^{-1}$, ϵ(nonG4) = 269000 $M^{-1}\cdot cm^{-1}$. Synthesis of **ZnP1** was described previously (22). Stock solutions of **ZnP1** (50 μM or 5 mM) were prepared by dissolving the dry compound in water. Dimethyl sulfate (DMS), polyethylene glycol (PEG) 200 and formamide were purchased from Sigma-Aldrich (USA).

The G-quadruplex structure was formed in 10 mM phosphate buffer (pH 7.8) containing either 100 mM KCl or 100 mM NaCl or 100 mM KCl supplemented with 40% PEG 200 via fast annealing: the solution of the oligonucleotide was heated for 1 min at 95°C followed by 10 min incubation on ice. The duplex structure was obtained by mixing equimolar amounts of TQ23-F and TQ23comp oligonucleotides in 10 mM phosphate buffer (pH 7.8) containing 100 mM KCl and heated for 1 min at 95°C with a subsequent slow cooling to room temperature for 2 h. ZnP1 was added from a stock solution to a pre-formed DNA structure after a renaturation procedure in all experiments.

Light source

To avoid heating of the samples and ensure an equal illumination dose when irradiating multiple samples, we used a set of blue (460–470 nm) light-emitting diodes (LED; luminous intensity 2 cd, bulb size 5 mm). Each LED was intended to irradiate a single sample having been applied directly to the bottom of the tube.

Fluorescence and absorption spectroscopy

FAM quenching was registered with a Cary Eclipse spectrofluorometer (Varian) at a wavelength of 515 nm upon excitation at 490 nm. The measurements were conducted at 1 nM of oligonucleotide. Apparent binding constants were estimated by fitting experimental data to a 1:1 stoichiometry model binding curve. Absorption spectra were recorded with a Jasco V-550 spectrophotometer in the 350–700 nm wavelength range. Absorbance spectra were obtained for the sequential mixture of 2 μM TQ23 oligonucleotide and 2 μM **ZnP1** solutions at different ratios. Thus, the total concentration of TQ23+**ZnP1** was constant equalling 2 μM.

Isothermal titration calorimetry (ITC)

The thermodynamic parameters of **ZnP1** binding to TQ23 oligonucleotide were measured using an iTC200 instrument (MicroCal, Northampton, MA, USA). Experiments were carried out at 25°C in 10 mM sodium phosphate buffer (pH 7.8) supplemented with either 100 mM NaCl or 100 mM KCl or 100 mM KCl with 40% PEG 200. Two microliter aliquots of 500 μM **ZnP1** solution were injected into a 200 μl calorimetric cuvette containing 20 μM of oligonucleotide in an appropriate buffer solution to achieve the complete binding isotherm. The heat of dilution was measured by injecting a solution of **ZnP1** into the same buffer. The obtained values were subtracted from the heat of binding reaction to obtain the effective heat of binding. The resulting titration curves were fitted to two-binding-mode model using MicroCal Origin software. Thus, the association constant (K), enthalpy change (ΔH) and stoichiometry (N), were determined. The entropy variation (ΔS) was calculated according to the standard thermodynamic equation. Three independent experiments were averaged.

CD spectroscopy

Circular dichroism (CD) measurements were performed at 20°C with a Jasco-715 CD spectrometer using a quartz cell with a 10 mm optical path length. The spectra were obtained at a bandwidth of 1 nm. Three scans were averaged. The concentration of oligonucleotides was 2 μM. CD at 290 nm was chosen for plotting the temperature denaturation curves. The melting curves were normalized to CD signal at 20°C corresponding to a completely folded structure. The temperature ramp was 0.5°C/min. Melting temperature was determined as the midpoint of the curve.

Mass spectrometry

Before MALDI MS analysis, the reaction mixture was desalted using C-18 ZipTip (Millipore, USA) according to the protocol recommended by the manufacturer. Reaction products were applied to the MALDI plate with 2 μl of 30% acetonitrile. For MALDI MS analysis of oxidation products, 3-hydroxypicolinic acid (3HPA) diluted in deionized water (35 mg/ml) was used as a matrix. A 0.2 M stock solution of diammonium citrate diluted in deionized water was added to the 3HPA matrix for a final concentration of 10 mM that maintained the molecules in an ammonium form. MALDI-TOF MS scans were performed using MicroFlex instrument (Bruker, Germany) equipped with a nitrogen laser (337 nm) for the detection of positive ions.

Nuclear magnetic resonance (NMR)

Samples for NMR analysis were prepared by fast renaturation of the TQ23 oligonucleotide at a concentration of 40 μM in a 0.55 ml solution of 90% H_2O:10% D_2O consisting of a 10 mM phosphate buffer (pH 7.8) and 100 mM KCl in the absence/presence of 20 μM **ZnP1**. One dimensional proton spectra of the samples in H_2O+D_2O were recorded with Bruker AVANCE III HD 300 MHz and Bruker AMX-III 400 MHz using Watergate W5 pulse sequence with gradient (zggpw5 from Bruker library) for efficient H_2O suppression. ^{1}H chemical shifts were referenced relative to external sodium 2,2-dimethyl-2-silapentane-5-sulfonate. Acquisition time was 12 h for a single 1D experiment. The NMR data were processed using Bruker XWIN-NMR and Bruker TopSpin 3.1 software.

Photocleavage with ZnP1 and DMS probing

DNA oxidation was performed in a 20 μl solution formed by mixing **ZnP1** porphyrin and pre-annealed TQ23-F oligonucleotide for a final concentration of 1 μM of ligand and 2 μM of TQ23-F. The reaction mixture was incubated for 10 min at room temperature prior to light irradiation for 1 min. DMS probing was performed by adding 1 μl of DMS (1:5 diluted in EtOH) to 20 μl of 2 μM TQ23-F preliminary renatured in the indicated buffer followed by incubation for 2 min at room temperature. After either **ZnP1**-induced oxidation or DMS modification, the oligonucleotide was EtOH-precipitated and dissolved in 4 μl of the loading buffer containing 30 mM sodium phosphate buffer (pH 7.8), 80 % formamide, 0.025 % bromophenol blue and 0.025 % xylene cyanol. Following the heating of the oligonucleotide in the loading buffer at 90°C for 20 min, the cleavage products were resolved in denaturing 16% polyacrylamide gel. The gel was visualized with Typhoon FLA 9500 fluorescence scanner (GE Healthcare, USA) equipped with 473 nm blue LD laser and LBP filter.

The above protocols for ZnP1 or DMS probing have been devised in our lab in order to adapt the conventional technique to fluorescently labeled oligonucleotides. We found that the use of the 3′-end fluorescent label (FAM) affords several benefits: (i) the 3′-end label enables the replacement of piperidine with other aqueous and non-aqueous solutions with formamide appearing to be the most efficient among those tested by us (similar observations were made recently by Stevens *et al*. (27)), (ii) the sequence of the short TQ23 oligonucleotide can be resolved entirely up to the last 3′-end nucleotide even in a small gel due to the low mobility of FAM label and high resolution of modern fluorescent scanners.

RESULTS

Quadruplex conformation remains intact upon ZnP1 binding

We started the study of interaction between **ZnP1** porphyrin and telomeric DNA with the analysis of structural effects that the ligand might induce in the telomeric DNA quadruplex upon binding. The inherent structural diversity of the human telomeric sequence was represented in this study by three conformations (Scheme 1) obtained by placing the oligonucleotide TQ23 under three types of solution conditions: presence of potassium ions, presence of sodium ions and under molecular crowding conditions.

Corresponding CD spectra of the TQ23 structures are shown in Figure 1 (blue spectra, open circles). The major conformation of TQ23 in the solution containing potassium ions was shown by NMR (4) to be the (3+1) Form 1 of the telomeric G-quadruplex (Scheme 1A). The corresponding CD spectrum consists of a positive band near 290 nm, a shoulder at 265 nm and a small negative band at

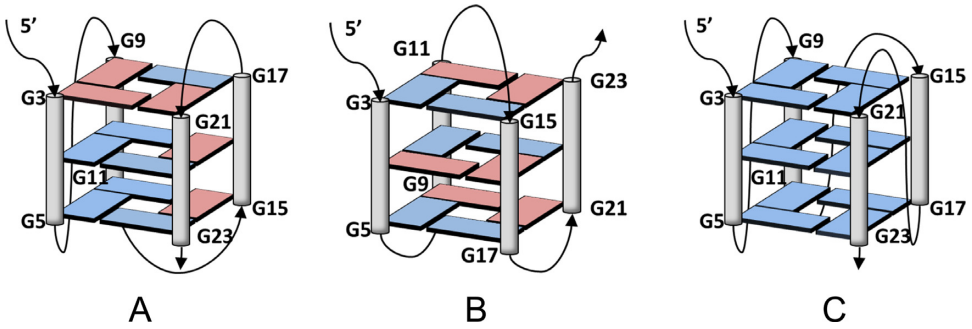

Scheme 1. Schemes of (3+1) Form 1 (A), antiparallel (**B**) and parallel (**C**) G-quadruplex conformations. Nucleotide numbering corresponds to TQ23 oligonucleotide. *Syn- and anti*-conformation of guanines are colored in pink and blue respectively.

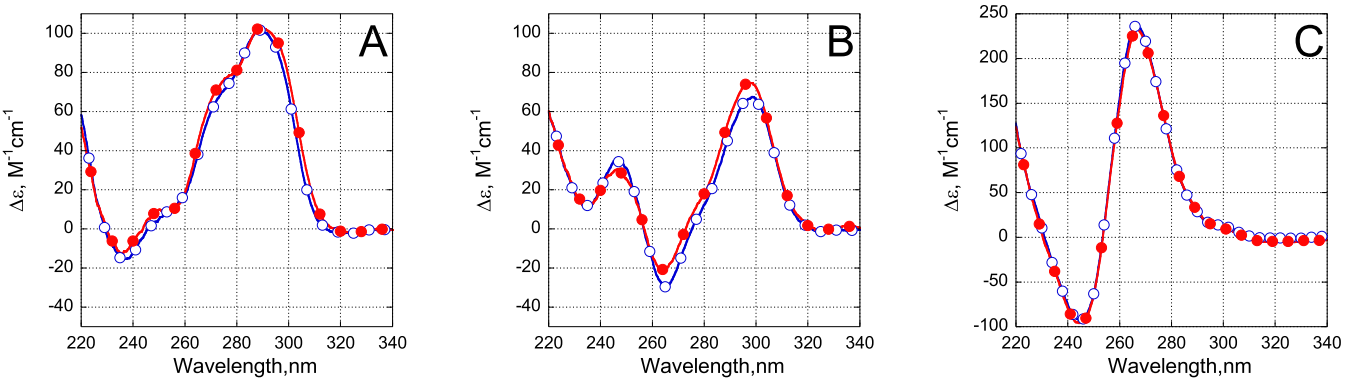

Figure 1. CD spectra of the telomeric oligonucleotide TQ23 in the presence of (**A**) K+ ions, (**B**) Na+ ions ions and under conditions of (**C**) molecular crowding. Blue open circles—spectra of G-quadruplex structure formed by TQ23 oligonucleotide; red filled circles— spectra in the presence of an equimolar concentration of **ZnP1** compound. The concentration of both TQ23 and **ZnP1** was 2 μM.

240nm (Figure 1A, blue spectrum, open circles). CD spectrum of the sodium-induced conformation (Figure 1B) has a positive band near 295 nm and a negative band at 265 nm, which is characteristic to an opposite stacking interaction of guanine quartets in antiparallel (Scheme 1B) G-quadruplex structure (28,29). Under molecular crowding conditions, TQ23 forms all-parallel G-quadruplex (Scheme 1C) and the CD spectrum has a positive band at 265 nm and a negative band at 240 nm (9) (Figure 1C).

The addition of an equimolar concentration of **ZnP1** compound did not change the CD spectra of the G-quadruplex structures (Figure 1, red spectra, filled circles). Further incubation of either TQ23 conformation with **ZnP1** also had no effect on the CD spectra, implying that drug binding does not disturb the DNA structure.

The hybrid (3+1) structure of the telomeric DNA is a family that includes 4 structural conformers with different loop arrangements but presumably similar CD spectra (4,6). One-dimensional ^{1}H NMR spectra were recorded in potassium salt in order to exclude possible structural transitions between different conformers within the hybrid (3+1) family upon binding with **ZnP1** (Figure 2). NMR spectrum of TQ23 in the absence of **ZnP1** porphyrin corresponds to the hybrid (3+1) Form 1 conformer of the telomeric G4 as described by Luu *et al.* (4). In the presence of **ZnP1**, broadening of resonance peaks and negligible changes of their chemical shifts caused by a complex formation with the ligand were observed. Most importantly, the shape of the spectrum and the positions of the peaks were mainly preserved indicating the conservation of the (3+1) Form 1 quadruplex conformation upon interaction with **ZnP1**.

ZnP1 binding sites on telomeric quadruplex

Parameters of the **ZnP1** interaction with TQ23 quadruplex were measured with ITC. The binding curves are biphasic (Supplementary Figure S2), showing the formation of two types of complexes with different stoichiometry and affinities. Fitting the theoretical binding curve of the two binding modes to the titration data enabled us to determine the thermodynamic parameters of binding (Table 1). The strongest **ZnP1** binding had a 1:1 stoichiometry for both sodium and potassium structures although the binding was characterized by a much higher binding constant in the case of the (3+1) Form 1 quadruplex (in the presence of K+ ions) as compared to the sodium-induced TQ23 structure (Na+ ions). Furthermore, weaker types of complexes were observed for both conformations. Three **ZnP1** molecules in potassium conditions and two **ZnP1** molecules in sodium conditions were able to bind to TQ23 with the constants measuring an order of magnitude smaller than that for the strong type complex. Stoichiometry of strong **ZnP1** binding to the parallel TQ23 in PEG had a peculiar feature: the stoichiometry of **ZnP1**:TQ23 interaction was close 1:2 (Table 1, bottom line). It may be accounted for the binding of a single **ZnP1** molecule to two adjacent parallel TQ23 quadru-

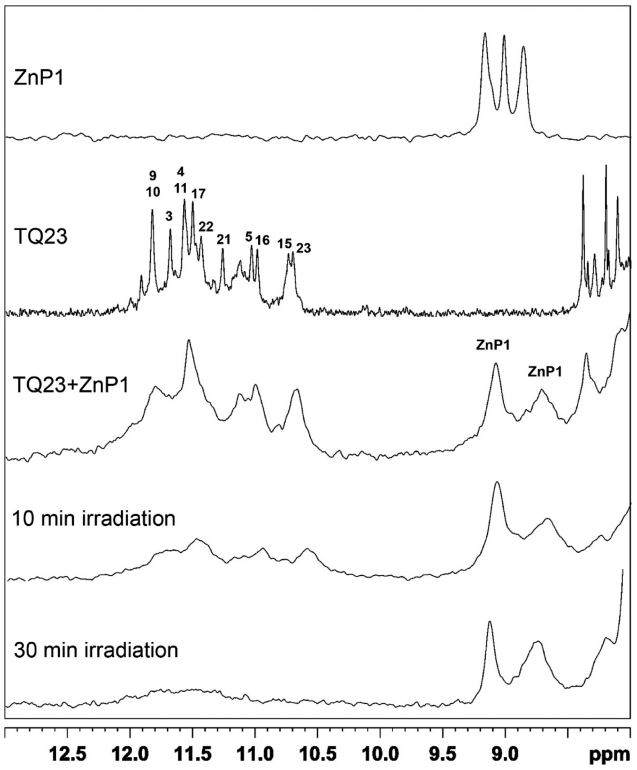

Figure 2. Imino and part of aromatic regions in ^{1}H NMR spectra of **ZnP1**, telomeric oligonucleotide TQ23 and complexes of TQ23 with **ZnP1**. The peaks corresponding to imino protons of TQ23 are assigned according to (4).

plexes. The dominance of the entropic component of the total free energy of **ZnP1** binding to all three G-quadruplex conformations suggests that hydrophobic interactions contribute significantly to binding.

The binding of **ZnP1** was further monitored by changes to its absorption spectra (Soret band) upon binding to the three G4 conformations of TQ23. The most profound bathochromic shift was observed in the case of the potassium G4 conformer at a low **ZnP1**:TQ23 ratio (Supplementary Figure S3) when the strong binding site was preferably occupied. This type of change in absorption spectra is indicative of the ligand shielding from solvent and therefore indicates stacking interaction in the strongest complex of **ZnP1** with G4 structure under potassium conditions.

The preferential position of the **ZnP1** binding site in TQ23 quadruplex was also probed by attaching FAM covalently either to the 5′ or to the 3′-end of TQ23 (oligonucleotides F-TQ23 and TQ23-F, correspondingly). The position of the strongest binding site for **ZnP1** porphyrin was assessed by monitoring of fluorescence quenching upon titration of F-TQ23 and TQ23-F at a low concentration (1 nM) of the oligonucleotides. We found that **ZnP1** quenches the 5′-FAM at a markedly smaller concentration than it does the 3′-FAM (Supplementary Figure S4). Therefore, the strongest binding site is closer to the 5′-end of the studied oligonucleotide folds. Note, the covalent attachment of FAM to either end of TQ23 does not change the quadruplex conformation as revealed by CD measurements (Supplementary Figure S5). In agreement with ITC data, the fluorescent method proved that the hybrid (3+1) structure has the highest affinity for **ZnP1** among the three G-quadruplex folds considered.

Light-induced conformational changes in telomeric G4 structure

Porphyrins are known to modify nucleic acids by generating reactive oxygen species when exposed to light. This property of porphyrins was tested for **ZnP1** in complex with the three G4 conformations under study. Illumination of **ZnP1**:TQ23 complex with blue light (see Materials and Methods) led to significant CD spectral changes for TQ23 oligonucleotide in potassium and for molecular crowding conditions. According to CD measurements, both the (3+1) and the parallel G4 conformers (Figure 3A and C, correspondingly) tended to transform to an antiparallel type of structure. On the contrary, sodium-induced structures retained conformation upon irradiation of the complex with **ZnP1** (Figure 3B). In the control experiment, no changes of TQ23 CD spectra upon light illumination in the absence of **ZnP1** was detected (Supplementary Figure S6).

Similar conformational changes were observed for the interaction of the telomeric quadruplex with the ligands PDS, 360A and phen-DC3 (12). Authors interpreted the observed CD spectral changes in terms of a structural rearrangement of the (3+1) form to an antiparallel G4 caused by the displacement of a K^+ ion from the quadruplex. In our case, the binding of the ligand left the structure intact, however, subsequent irradiation with light resulted in the formation of the structure with CD spectrum typical for an antiparallel G4 both in 100 mM KCl and in the presence of 40% PEG 200 with 100 mM KCl (green curves in Figure 3A and C).

Light-illumination of the complex **ZnP1**:TQ23 in a potassium buffer for 30 min resulted in the disappearance of the NMR peaks corresponding to the imino proton transfer in the G4 structure (Figure 2, two bottom spectra). Evidently, the appearance of the oxidation products of guanine nucleotides seems to have led to the destruction of some guanine quartets and the subsequent refolding to a more favorable TQ23 conformation. Since different guanines can be oxidized in different G4-molecules, light-illumination can result in heterogeneous mixture of G-quadruplex molecules of TQ23 characterized by antipar-

Table 1. Thermodynamic parameters of **ZnP1** binding with TQ23 quadruplex

	N_1	K_1, 10^6 M^{-1}	ΔH_1, kcal/mol	$-T\Delta S_1$, kcal/mol	N_2	K_2, 10^6 M^{-1}	ΔH_2, kcal/mol	$-T\Delta S_2$, kcal/mol
K^+	1.0 ± 0.1	130 ± 90	−2.0 ± 0.1	−9.0	3.1 ± 0.1	5 ± 4	−0.33 ± 0.03	−8.8
Na^+	0.8 ± 0.1	3.7 ± 1.5	−2.9 ± 0.2	−6.0	2.1 ± 0.2	0.3 ± 0.1	−0.9 ± 0.2	−6.5
K^+/PEG	0.4 ± 0.1	15 ± 6	−3.4 ± 0.2	−6.3	2.5 ± 0.1	6.6 ± 0.3	−0.66 ± 0.08	−7.2

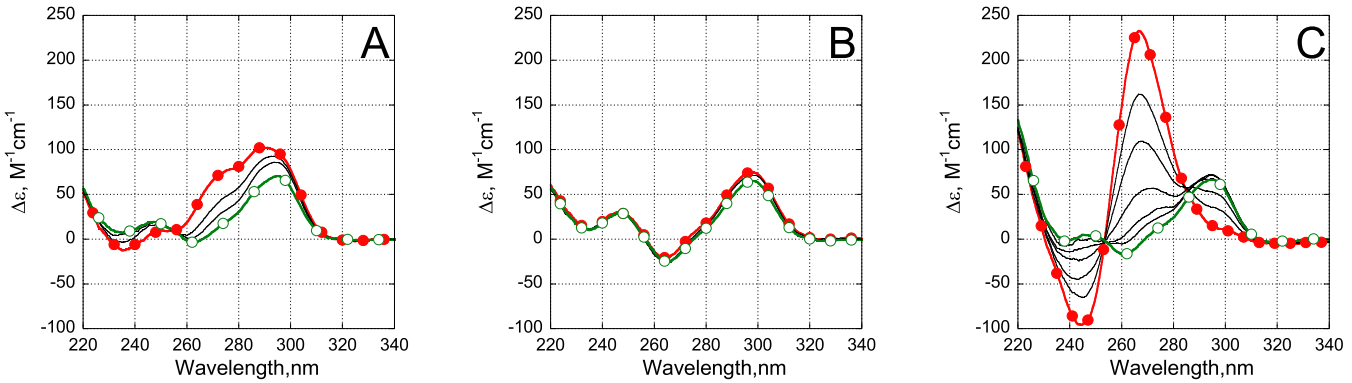

Figure 3. Changes of circular dichroism spectra after light irradiation of telomeric oligonucleotide TQ23 and **ZnP1** complex in the presence of (**A**) K+ ions and (**B**) Na+ ions and under (**C**) molecular crowding conditions. Red spectra correspond to the equimolar mixture of TQ23 oligonucleotide and **ZnP1** before irradiation (red, circles); Black not marked spectra were recorded after illumination with blue light for (A and B) 5 and 10 min and (C) 5, 10, 20, 30, 45 min. Green open circles - spectra after illumination with blue light (A –20 min; B – 20min; C – 60 min).

allel type of CD spectrum (to be discussed below in more detail). At the same time, **ZnP1** seems to remain bound to the resulting conformations of TQ23 since: (i) positions of **ZnP1** aromatic peaks practically do not shift after light illumination (Figure 2), and (ii) the environment of **ZnP1** changes insignificantly after irradiation of the **ZnP1**:TQ23 complex as judged by minor alterations of **ZnP1** absorption spectrum (Supplementary Figure S7).

Thermodynamic stability of the G4 structure initially increases upon formation of the complex with **ZnP1** yet then decreases considerably (ΔTm = 15°C) after light-irradiation of the complex (Supplementary Figure S8). Earlier, Vorlickova *et al*. demonstrated that direct synthetic replacement of certain guanines with 8-oxo-guanines in the telomeric quadruplex leads to the destabilization of the structure (30). In order to define the position of the modified guanines and the type of modification induced by **ZnP1**, we performed chemical mapping and MS analysis.

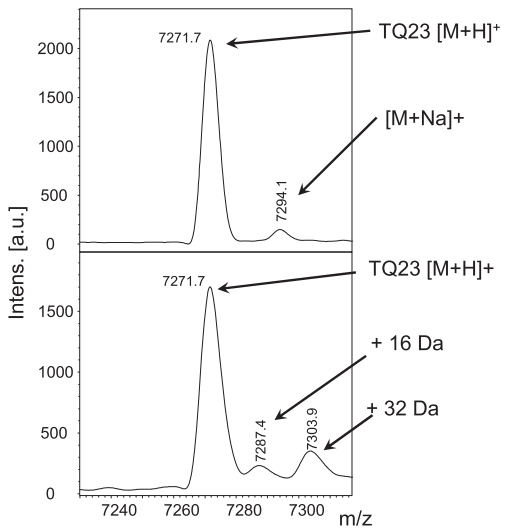

Figure 4. MALDI MS spectra of **ZnP1**:TQ23 complex in potassium-containing buffer before (top) and after 5 min of light irradiation (bottom).

Sp and 8oxoG are the two major forms of guanine light-induced modifications by ZnP1

The products of guanine oxidation were analyzed by MALDI-TOF mass spectrometry. Figure 4 shows MALDI MS spectra for the reaction mixture with an equimolar **ZnP1** concentration without light-illumination (top) and after a short exposure to light (bottom). Two signals, with +16 Da and +32 Da, of oxidized oligonucleotide were the most intense in the analyzed reaction mixture. The +16 Da band corresponds most likely to 8-oxoG, while the +32 Da band may indicate either the simultaneous oxidation of two guanines to their 8-oxo form, or the formation of another oxidation product, spiroiminodihydantoin, which contributes to an additional +32 Da shift on the molecular weight of the original oligonucleotide (15). Since the oxidation was performed in mild conditions (5 min of irradiation to the complex) and only a small fraction of molecules were supposed to get oxidized, simultaneous modification of two guanines was very unlikely for statistical reasons. Hence, we assigned the +32 Da peak to the spiroiminodihydantoin oxidation product.

Mapping of the oxidized guanines in TQ23 sequence

Guanine oxidation of the telomeric oligonucleotide TQ23-FAM was performed in five different structural contexts: unfolded DNA (ssDNA), double stranded DNA (dsDNA) and three types of the G-quadruplex conformations mentioned above. ssDNA was obtained by heating and subsequent fast cooling of the oligonucleotide in 20 mM Tris HCl buffer (pH 8.0) without the addition of any counterions. A CD spectrum of TQ23 confirmed that the oligonucleotide was poorly structured under these experimental conditions (Supplementary Figure S9). dsDNA was annealed slowly in presence of the complementary oligonucleotide, TQ23comp, while potassium-, sodium- and PEG-induced G4 conformations were formed as described above. Attachment of the 3′-FAM label did not change any of the G4 conformations as demonstrated above by CD (Supplementary Figure S5). Treatment of the TQ23-FAM with DMS confirmed proper formation of all five types of structures under the indicated conditions: ssDNA (Figure 5

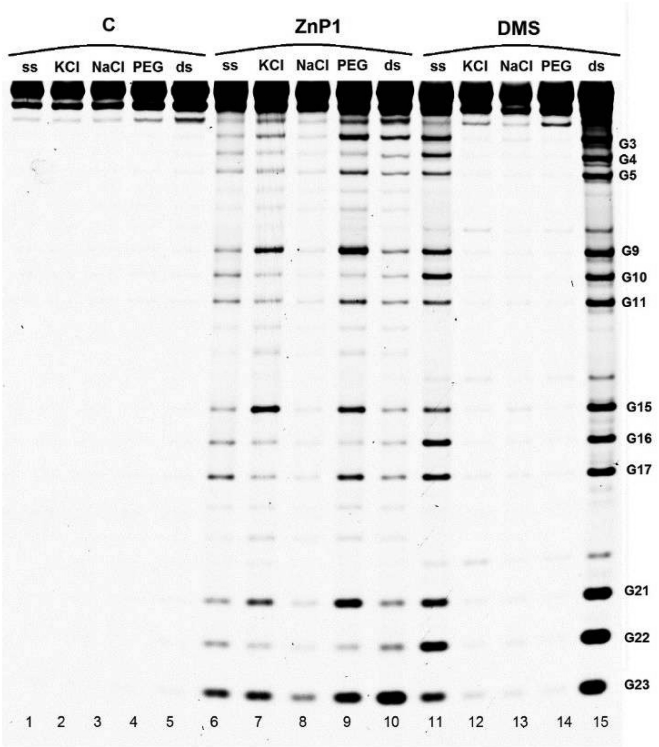

Figure 5. Modification of TQ23-FAM with **ZnP1** (lanes 6–10) or DMS (lanes 11–15). Five structural forms of TQ23 (see text) was probed: unfolded DNA (ss), G4 potassium form (KCl), G4 sodium (NaCl), G4 in KCl/PEG (PEG) and double stranded DNA (ds). C-control lanes obtained by the same light irradiation in the absence of **ZnP1** (lanes 1–5).

lane11) and dsDNA (Figure 5, lane 15) were modified with DMS, while the three G4 DNA conformations were protected from DMS modification as expected (Figure 5, lanes 12–14).

For **ZnP1** probing experiments, the ligand was added to each pre-formed structure, incubated for 10 min and then briefly light irradiated to ensure partial DNA modification. Subsequent cleavage of the TQ23 oligonucleotide at the oxidized guanines showed that each structural form of the oligonucleotide displayed a specific pattern of guanine modification. ssDNA and dsDNA demonstrated weak and nearly uniform oxidation of all the guanines in the TQ23 oligonucleotide (Figure 5, lanes 6 and 10, correspondingly). In the presence of 100 mM KCl, certain guanines of the extreme tetrads were modified. Modifications of the G9 and the G15 were most profound while that of the G3, G23 and G21 were less explicit (Figure 5, lane 7). In presence of 40% PEG 200, the guanines at the 5′-end of each GGG block were the most efficiently oxidized guanines; a weaker oxidation occurred to the guanines of the 3′- tetrad while the middle tetrad remained untouched (Figure 5, lane 9). The higher oxidation efficiency of the guanines belonging to flanking G-quartets can be interpreted by their greater accessibility to the solvent. This is supported by the uniform modification of all Gs in duplex and in non-structured DNA, where the nucleotides are equally accessible.

Light-induced modification of the TQ23 with **ZnP1** appeared ineffective for sodium-induced G-quadruplex structure. This effect cannot be explained solely by the lower affinity of **ZnP1** to the sodium telomeric G4 conformation, as the light-induced modification was performed at concentrations of both oligonucleotide and the drug exceeding dissociation constant of the interaction. Other factors should be considered to provide a possible explanation, e.g. a lower solvent accessibility of guanines in the sodium structure or a different type of the ligand interaction with sodium TQ23 conformation.

One can also note that the G23 which is located at the very 3′-end of the oligonucleotide displayed a higher reactivity independent of the structure. This effect can be due to a higher solvent accessibility of the G23 residue because of an inherent flexibility of the 3′-end bearing fluorescent label FAM. In order to exclude FAM-dependent photo-inducible modification of the nearby Gs, we performed a control experiment in the absence of **ZnP1** (Figure 5, lanes 1–5). Since no oxidation of the FAM-labeled oligonucleotide was observed in this case, we can conclude that guanine modifications arise exclusively from **ZnP1**-driven photo-oxidation of DNA. Thus, the pattern of the G4 photo inducible oxidation in the presence of **ZnP1** is specific to each telomeric quadruplex conformation.

Since neither 8-oxoG nor Sp can maintain the proper structure of the G-tetrad (30), oxidation of any of the G3, G9, G15, G21 or G23 in a KCl solution should lead to destruction of the tetrad this guanine belongs to. The other three guanines of the tetrad may still form a triplet or disintegrate. The two remaining tetrads may also stay intact or rearrange after oxidation. In an attempt to shed some light on how the oxidation of a guanine affects the overall G4 structure, we performed DMS probing of the TQ23 G4 structure after light-induced modification with **ZnP1** (Supplementary Figure S10). This experiment reveals the guanines that are still protected by Hoogsteen interactions after the oxidation.

When performed in a KCl solution (Supplementary Figure S10, lanes 2–4), the probing experiment clearly shows that after oxidation with **ZnP1**, the guanines belonging to the extreme tetrads are more strongly modified by DMS than the guanines belonging to the middle tetrad (Supplementary Figure S10, lane 4). Although we probed with DMS a mixture of different molecules that may have different guanines oxidized, we can conclude, that all of them have the middle tetrad intact, while either the top or bottom tetrad are disturbed by oxidation. The same probing experiment was performed in sodium (Supplementary Figure S10, lanes 5–7) and confirmed that the sodium structure was less susceptible to oxidation, remaining largely intact and protected from DMS modification. One may conceive that such a resistance of the sodium structure to **ZnP1** oxidation may be attributed to the nature of the counter ion. To address this, we tested the efficiency of **ZnP1**-dependent oxidation of an unrelated to G4 structure oligonucleotide nonG4: AGGCTTGGCGGGAAAAAGAACG in sodium and potassium buffer solutions (Supplementary Figure S10, lanes 8 and 9). Five minutes of light irradiation of the single-stranded oligonucleotide revealed identical oxidation efficiency of guanines in the different salts.

Therefore, the poor oxidation of the sodium conformation in TQ23 is determined by its idiosyncratic structure

and its peculiar way of interaction with the ligand. We compared the **ZnP1**-dependent oxidation of the sodium form of 23-mer TQ23 with that of the 22-mer TQ22 AG3(TTAG3)3 presenting an antiparallel structure established by both NMR and CD methods (2,29). The light-induced changes of the **ZnP1** complexes with TQ23 and TQ22 were monitored by CD measurements (Supplementary Figure S11) and by mapping of the modified guanines (Supplementary Figure S12). CD revealed that in spite of the deeper band at 260 nm, the antiparallel sodium structure of TQ22 behaved similarly to the sodium structure of TQ23: binding of **ZnP1** to TQ22 or TQ23 in Na+ and subsequent light irradiation have not resulted in any remarkable changes of the CD spectra (Supplementary Figure S11). In agreement with CD, probing of the oxidized guanines showed that, similar to the sodium form of TQ23 oligonucleotide, antiparallel TQ22 structure is resistant to light-induced oxidation (Supplementary Figure S12). Thus, we conclude that the distinctive oxidation patterns of the studied G-quadruplex folds reflect their structural topology.

DISCUSSION

In this work we analyzed the interaction of porphyrin derivative **ZnP1** with three conformations of the telomeric G-quadruplex DNA formed by oligonucleotide d(TAGGG(TTAGGG)$_3$) (TQ23). Contrary to the majority of G-quadruplex specific ligands, **ZnP1** appeared not to disturb intact structures of the G-quadruplex as demonstrated by CD and NMR. Three independent techniques – ITC, **ZnP1** absorption and fluorescent quenching were applied to access an affinity and character of the ligand binding to the G-quadruplex conformations. We observed two types of complexes, a strong and a weak one and a considerable entropy contribution to the free energy of binding. The potassium-induced structure revealed a higher affinity and higher entropic component than the sodium-induced structure. The entropy-driven binding of other porphyrin derivatives to a quadruplex was observed earlier (20) and could be explained by the large hydrophobic surface of the porphyrin ring available for interaction with DNA. Data for TMPyP4 (20) suggests that TMPyP4 molecules could bind to the truncated human quadruplex sequences, both in potassium and under molecular crowding conditions, via two distinct stacking-mode interactions: with the external G-tetrad planes and with the bases of the loops connecting the G-tetrads. Previously, (24) we had found that the interaction of the metal-free tetra-carboxymethyl porphyrin analogue P1 with the sodium form of the telomeric quadruplex results in two types of complexes: a strong complex can occur from the interaction with TTA loops whereas the weaker complexes are formed with G-quartets. Evidently, the preferable mode choice of porphyrin binding to G4 DNA (stacking with G-quartets or interaction with loops) is defined by several factors: the type of G4 conformation, the substituents on the porphyrin periphery (carboxymethyl groups in our case) and the presence of a metal-ion in its macrocycle.

In case of **ZnP1** porphyrin, quenching experiments of the 5′- and 3′- fluorescently labeled oligonucleotide TQ23 (Supplementary Figure S4) argue that the preferential site of binding is located within the vicinity of the 5′-end of the oligonucleotide regardless of the type of TQ23 folding: potassium or sodium G4 forms. However, several lines of evidence suggest that the interaction of **ZnP1** with potassium and sodium G4 conformations have different characters. Stronger affinity, higher entropy contribution to the binding free energy, a considerable shift of absorption spectra of **ZnP1** under potassium conditions may suggest direct stacking interactions of the ligand with the 5′ G-quartet of the (3+1) form. At the same time, decreased entropic components of the interaction with **ZnP1**, a negligible shift in the Soret band upon ligand binding and resistance of the sodium structure to **ZnP1**-dependent oxidation assume a different type of interaction by the sodium structure with the ligand. We can suggest that the sodium conformation accommodates **ZnP1** mainly by the loops. The bases of the loops could be involved in stacking interactions with **ZnP1** in a similar fashion as observed in the X-Ray structure of the TMPyP4 complex with G4 DNA (31), which would explain still notable entropy contribution to free energy of **ZnP1** binding to the sodium structure. Resistance of the sodium conformer to **ZnP1**-dependent oxidation can be explained by a distal interaction of the ligand with the loops, which set the ligand apart from the core of the G4 structure and prevent generated singlet oxygen from reaching the guanines. Antiparallel topology of the sodium form of TQ23 (conforming with its typically antiparallel CD spectrum) would promptly explain its lower affinity to the drug: the interaction could be constrained, e.g. by presence of the diagonal loop that could protect the 5′-G-quartet from stacking with **ZnP1.** Our comparison of the oxidation efficiency of TQ23 and TQ22 showed that the sodium forms of both oligonucleotides are resistant to oxidation while their potassium forms are more sensitive to **ZnP1**-dependent oxidation. Similar resistance to **ZnP1**-dependent oxidation for sodium forms of TQ23 and the antiparallel structure of TQ22 implies similar conformation for both oligonucleotides.

Summarizing the experimental data, we conclude that such a distinct behavior of the sodium and potassium forms of TQ23 should originate from their structural dissimilarity. Wang *et al*. showed by NMR that oligonucleotide TQ23 folds in (3+1) Form 1 structure both in KCl and NaCl solution, despite different CD and 1D NMR spectra (7). If we assume that at low (micromolar) concentrations, both sodium and potassium structures of TQ23 have the same (3+1) topology, then it would be difficult to explain remarkably altered mode of interaction of these conformers with **ZnP1** by local differences in the tetrads stacking or tensions in the loops brought about by sodium ions. On the other hand, several studies have demonstrated that a high oligonucleotide concentration coupled with prolonged incubation of the telomeric G-DNA may cause a tremendous change of the initial structure (32–34). We believe that the diverse solution conditions of low (this study) and high (NMR) oligonucleotide concentrations as well as applied renaturation procedures may cause the inconsistency. We have provided several lines of experimental evidence that suggests the presence of a predominantly antiparallel conformation of sodium form in TQ23 under our experimental

conditions. Thus, light-induced action of **ZnP1** porphyrin on the telomeric G-quadruplex reflects a topology of G-quadruplex folding.

Although the mechanism of **ZnP1** action on the telomeric DNA is not known, we can hypothesize on the nature of the G4 structural changes occurring after light-induced oxidation. Since binding of **ZnP1** to G4 DNA does not change its conformation, we conclude that the modification of guanines occurring after irradiation is the main driving force of the conformational changes. According to mapping of TQ23 modification in KCl, several guanines (G3, G9, G15, G21 or G23) of the external tetrads can be oxidized under light irradiation. This experiment is done under conditions when only a small fraction of the DNA molecules are modified, i.e. no more than one guanine is modified per molecule. Consequently, we obtain a mixture of the telomeric G4 molecules with different guanines oxidized. Such heterogeneity makes determining the resulting structure with NMR impossible although the resulting mixture is characterized by antiparallel type of circular dichroism spectrum (Figure 3A, green spectrum). We suppose that regardless of position of modification (G3, G9, G15, G21 or G23), all these different G-quadruplex molecules tend to rearrange into antiparallel G4 conformation. This is supported by works of Vorlickova *et al*. (30) and Zhou *et al*. (18), demonstrated that modification of any single guanine of the extreme tetrads is sufficient for triggering certain conformational changes resulted in a final structure with antiparallel type of CD spectrum.

Oxidation of any guanine G3, G9, G15, G21 or G23 (schematically depicted in Figure 6A in red) in KCl disturbs either the top or bottom tetrad. Although the C8 atom is not involved in the interaction between the bases, it is located in the grooves and 8-oxo modifications may shift the preference of the base to adopt *syn* or *anti* conformation in G4 DNA. 8-oxoG(*syn*):A(*anti*) base pair (Figure 6B) is known to arise in double stranded DNA (35) and one can envision this type of interaction between 8-oxoG and an adenine of the loops. This interaction with the loops may include a strand shift as shown in the right column of Figure 6A. Note, that in the latter case, the middle tetrad (G4-G10-G16-G22) still remains intact, thus conforming to the DMS probing of the oxidized G4-DNA (Supplementary Figure S10). The other product, spiroiminodihydantoin must destroy the G-tetrade, but can also create an alternative interaction to an adenine of the loops or a guanine (35,36) (Figure 6B) that could contribute to an energy gain necessary for conformational rearrangement. Additionally, a decrease in the terminal quartet stability leads to a loss of a hydrophobic surface, which may induce the switch to the resulting conformation (CD spectrum in green, Figure 3C).

Interestingly, the (3+1) potassium telomeric structure tends to change its CD spectra to an antiparallel type under a variety of other factors. For example, the binding of several G4 specific drugs, e.g. 360A, Phen-DC3 and PDS (12) and cations (37) grant telomeric G4 DNA antiparallel conformation. Along with 8oxoG (30), adenine (38) or an abasic site (39) substitution for any guanine belonging to the terminal quartets had a similar effect according to the CD spectra.

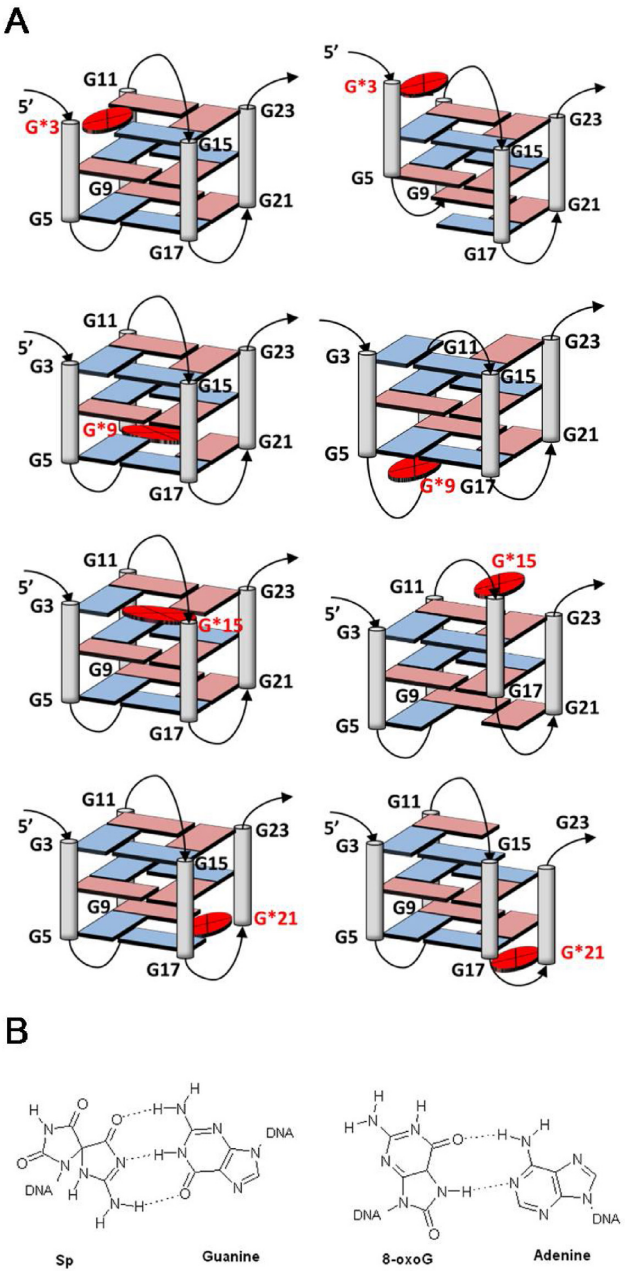

Figure 6. (**A**) Schematic illustration of different products of TQ23 arising after oxidation of one of the guanines G3, G9, G15, G21 in KCl solution by ZnP1 under light irradiation. The oxidized G residue (8-oxoG or Sp) is depicted in red. Although the mechanism of tetrads rearrangement after bulging out of the oxidized G is not known, a shift of the strand containing oxidized guanine base might be involved as illustrated in the right column structures. (**B**) Hypothetical pairing of Sp with guanine and of 8-oxoG with adenine (35,36).

CONCLUSION

In this study, we have demonstrated that Zn(II) tetracarboxymethyl porphyrin derivative **ZnP1** is able to bind to different conformations of the G4 telomeric DNA: parallel, antiparallel and (3+1) conformations. Although **ZnP1** has different affinities and possible different modes of interaction with the three types of intramolecular telomeric

G-quadruplex, the ligand does not affect the native conformation of the G4 DNA upon binding. **ZnP1** preferentially modifies intramolecular (3+1) and parallel G4 conformations upon light-illumination producing a pattern of guanine cleavage specific to each conformation. This property may be applied in probing and structural characterization of the quadruplex fold in combination with other spectral data. Independent of the initial type of the telomeric G4 fold, light-induced oxidation of the G4 in complex with **ZnP1** results in a conformational rearrangement to an antiparallel type of G4 structure. Modification of guanines at the 5′-end of the telomeric sequence is known to be the most effective in telomerase inhibition (17). We further assume that the light-induced selective oxidation of the 5′-flanking guanines caused by the porphyrin derivatives have the potential to be used for reducing telomerase activity in tumor cells.

SUPPLEMENTARY DATA

Supplementary Data are available at NAR Online.

ACKNOWLEDGEMENTS

The authors thank the mass-spectrometry facility at the Institute for Physical-Chemical Medicine, Ministry of Public Health for assistance in MS analysis. The authors are deeply indebted to Janine Appleton for language editing.

FUNDING

Russian Science Foundation [project 16-14-10396]; part of this work (chemical probing, ITC, MS spectroscopy) was funded by the Russian Foundation for Basic Research [project 15-04-01748]. Funding for open access charge: Russian Science Foundation [project 16-14-10396].
Conflict of interest statement. None declared.

REFERENCES

1. Shay,J.W. and Bacchetti,S. (1997) A survey of telomerase activity in human cancer. *Eur. J. Cancer*, **33**, 787–791.
2. Wang,Y. and Patel,D.J. (1993) Solution structure of the human telomeric repeat d[AG3(T2AG3)3] G-tetraplex. *Structure*, **1**, 263–282.
3. Parkinson,G.N., Lee,M.P. and Neidle,S. (2002) Crystal structure of parallel quadruplexes from human telomeric DNA. *Nature*, **417**, 876–880.
4. Luu,K.N., Phan,A.T., Kuryavyi,V., Lacroix,L. and Patel,D.J. (2006) Structure of the human telomere in K+ solution: an intramolecular (3 + 1) G-quadruplex scaffold. *J. Am. Chem. Soc.*, **128**, 9963–9970.
5. Phan,A.T., Kuryavyi,V., Luu,K.N. and Patel,D.J. (2007) Structure of two intramolecular G-quadruplexes formed by natural human telomere sequences in K+ solution. *Nucleic Acids Res.*, **35**, 6517–6525.
6. Phan,A.T., Luu,K.N. and Patel,D.J. (2006) Different loop arrangements of intramolecular human telomeric (3+1) G-quadruplexes in K+ solution. *Nucleic Acids Res.*, **34**, 5715–5719.
7. Wang,Z.F., Li,M.H., Hsu,S.T. and Chang,T.C. (2014) Structural basis of sodium-potassium exchange of a human telomeric DNA quadruplex without topological conversion. *Nucleic Acids Res.*, **42**, 4723–4733.
8. Lim,K.W., Amrane,S., Bouaziz,S., Xu,W., Mu,Y., Patel,D.J., Luu,K.N. and Phan,A.T. (2009) Structure of the human telomere in K+ solution: a stable basket-type G-quadruplex with only two G-tetrad layers. *J. Am. Chem. Soc.*, **131**, 4301–4309.
9. Heddi,B. and Phan,A.T. (2011) Structure of human telomeric DNA in crowded solution. *J. Am. Chem. Soc.*, **133**, 9824–9833.
10. Gray,R.D., Trent,J.O. and Chaires,J.B. (2014) Folding and unfolding pathways of the human telomeric G-quadruplex. *J. Mol. Biol.*, **426**, 1629–1650.
11. Boncina,M., Vesnaver,G., Chaires,J.B. and Lah,J. (2016) Unraveling the thermodynamics of the folding and interconversion of human telomere G-quadruplexes. **55**, 10340–10344.
12. Marchand,A., Granzhan,A., Iida,K., Tsushima,Y., Ma,Y., Nagasawa,K., Teulade-Fichou,M.P. and Gabelica,V. (2015) Ligand-induced conformational changes with cation ejection upon binding to human telomeric DNA G-quadruplexes. *J. Am. Chem. Soc.*, **137**, 750–756.
13. Kaluzhny,D., Ilyinsky,N., Shchekotikhin,A., Sinkevich,Y., Tsvetkov,P.O., Tsvetkov,V., Veselovsky,A., Livshits,M., Borisova,O., Shtil,A. *et al.* (2011) Disordering of human telomeric G-quadruplex with novel antiproliferative anthrathiophenedione. *PLoS One*, **6**, e27151.
14. Bonnett,R. (1995) Photosensitizers of the porphyrin and phthalocyanine series for photodynamic therapy. *Chem. Soc. Rev.*, **24**, 19–33.
15. Fleming,A.M. and Burrows,C.J. (2013) G-quadruplex folds of the human telomere sequence alter the site reactivity and reaction pathway of guanine oxidation compared to duplex DNA. *Chem. Res. Toxicol.*, **26**, 593–607.
16. Wheelhouse,R.T., Sun,D., Han,H., Han,F.X. and Hurley,L.H. (1998) Cationic porphyrins as telomerase inhibitors: the interaction of tetra-(N-methyl-4-pyridyl) porphine with quadruplex DNA. *J. Am. Chem. Soc.*, **120**, 3261–3262.
17. Szalai,V.A., Singer,M.J. and Thorp,H.H. (2002) Site-specific probing of oxidative reactivity and telomerase function using 7,8-dihydro-8-oxoguanine in telomeric DNA. *J. Am. Chem. Soc.*, **124**, 1625–1631.
18. Zhou,J., Fleming,A.M., Averill,A.M., Burrows,C.J. and Wallace,S.S. (2015) The NEIL glycosylases remove oxidized guanine lesions from telomeric and promoter quadruplex DNA structures. *Nucleic Acids Res.*, **43**, 4039–4054.
19. Xodo,L.E., Cogoi,S. and Rapozzi,V. (2016) Photosensitizers binding to nucleic acids as anticancer agents. *Future Med. Chem.*, **8**, 179–194.
20. Martino,L., Pagano,B., Fotticchia,I., Neidle,S. and Giancola,C. (2009) Shedding light on the interaction between TMPyP4 and human telomeric quadruplexes. *J. Phys. Chem. B*, **113**, 14779–14786.
21. Berezin,M., Berezina,N., Semeikin,A. and V'yugin,A. (2007) Thermochemistry of solution of some quaternized derivatives of tetra(4-pyridyl)porphine in water. *Russ. J. Gen. Chem.*, **77**, 1955–1958.
22. Kovaleva,O.A., Tsvetkov,V.B., Mamaeva,O.K., Ol'shevskaya,V.A., Makarenkov,A.V., Dezhenkova,L.G., Semeikin,A.S., Borisova,O.F., Shtil,A.A., Shchyolkina,A.K. *et al.* (2014) Preferential DNA photocleavage potency of Zn(II) over Ni(II) derivatives of carboxymethyl tetracationic porphyrin: the role of the mode of binding to DNA. *Eur. Biophys. J.*, **43**, 545–554.
23. Kovaleva,O.A., Tsvetkov,V.B., Shchyolkina,A.K., Borisova,O.F., Ol'shevskaya,V.A., Makarenkov,A.V., Semeikin,A.S., Shtil,A.A. and Kaluzhny,D.N. (2012) The role of carboxymethyl substituents in the interaction of tetracationic porphyrins with DNA. *Eur. Biophys. J.*, **41**, 723–732.
24. Kovaleva,O.A., Shchyolkina,A.K., Mamaeva,O.K., Ol'shevskaya,V.A., Makarenkov,A.V., Semeikin,A.S., Shtil,A.A., Borisova,O.F. and Kaluzhny,D.N. (2013) Complexes of antiparallel telomeric G-quadruplex d(TTAGGG)4 with carboxymethyl tetracationic porphyrins. *Mol. Biol.*, **47**, 453–460.
25. Han,F.X., Wheelhouse,R.T. and Hurley,L.H. (1999) Interactions of TMPyP4 and TMPyP2 with quadruplex DNA. Structural basis for the differential effects on telomerase inhibition. *J. Am. Chem. Soc.*, **121**, 3561–3570.
26. Zheng,K.-w., Zhang,D., Zhang,L.-x., Hao,Y.-h., Zhou,X. and Tan,Z. (2011) Dissecting the Strand Folding Orientation and Formation of G-Quadruplexes in Single- and Double-Stranded Nucleic Acids by Ligand-Induced Photocleavage Footprinting. *J. Am. Chem. Soc.*, **133**, 1475–1483.
27. Stevens,A.J., Kennedy,H.L. and Kennedy,M.A. (2016) Fluorescence methods for probing G-quadruplex structure in single- and double-stranded DNA. *Biochemistry*, **55**, 3714–3725.
28. Gray,D.M., Wen,J.D., Gray,C.W., Repges,R., Repges,C., Raabe,G. and Fleischhauer,J. (2008) Measured and calculated CD spectra of

G-quartets stacked with the same or opposite polarities. *Chirality*, **20**, 431–440.
29. Randazzo,A., Spada,G.P. and da Silva,M.W. (2013) Circular dichroism of quadruplex structures. *Top. Curr. Chem.*, **330**, 67–86.
30. Vorlickova,M., Tomasko,M., Sagi,A.J., Bednarova,K. and Sagi,J. (2012) 8-oxoguanine in a quadruplex of the human telomere DNA sequence. *FEBS J.*, **279**, 29–39.
31. Parkinson,G.N., Ghosh,R. and Neidle,S. (2007) Structural basis for binding of porphyrin to human telomeres. *Biochemistry*, **46**, 2390–2397.
32. Abu-Ghazalah,R.M., Rutledge,S., Lau,L.W., Dubins,D.N., Macgregor,R.B. Jr and Helmy,A.S. (2012) Concentration-dependent structural transitions of human telomeric DNA sequences. *Biochemistry*, **51**, 7357–7366.
33. Li,Y.Y., Abu-Ghazalah,R., Zamiri,B. and Macgregor,R.B. (2016) Concentration-dependent conformational changes in GQ-forming ODNs. *Biophysical Chem.*, **211**, 70–75.
34. Renciuk,D., Kejnovska,I., Skolakova,P., Bednarova,K., Motlova,J. and Vorlickova,M. (2009) Arrangements of human telomere DNA quadruplex in physiologically relevant K+ solutions. *Nucleic Acids Res.*, **37**, 6625–6634.
35. David,S.S., O'Shea,V.L. and Kundu,S. (2007) Base-excision repair of oxidative DNA damage. *Nature*, **447**, 941–950.
36. Henderson,P.T., Delaney,J.C., Muller,J.G., Neeley,W.L., Tannenbaum,S.R., Burrows,C.J. and Essigmann,J.M. (2003) The hydantoin lesions formed from oxidation of 7,8-dihydro-8-oxoguanine are potent sources of replication errors in vivo. *Biochemistry*, **42**, 9257–9262.
37. Largy,E., Marchand,A., Amrane,S., Gabelica,V. and Mergny,J.L. (2016) Quadruplex turncoats: Cation-dependent folding and stability of quadruplex-DNA double switches. *J. Am. Chem. Soc.*, **138**, 2780–2792.
38. Tomasko,M., Vorlickova,M. and Sagi,J. (2009) Substitution of adenine for guanine in the quadruplex-forming human telomere DNA sequence G(3)(T(2)AG(3))(3). *Biochimie*, **91**, 171–179.
39. Skolakova,P., Bednarova,K., Vorlickova,M. and Sagi,J. (2010) Quadruplexes of human telomere dG(3)(TTAG(3))(3) sequences containing guanine abasic sites. *Biochem. Biophys. Res. Commun.*, **399**, 203–208.